2010 IEEE International Conference on Robotics and Automation
Anchorage Convention District
May 3-8, 2010, Anchorage, Alaska, USA

Global Reachability and Path Planning for Planetary Exploration with Montgolfiere Balloons

Lars Blackmore*, Yoshiaki Kuwata*, Michael T. Wolf*, Christopher Assad*,
Nanaz Fathpour*, Claire Newman† and Alberto Elfes*
*Jet Propulsion Laboratory, California Institute of Technology, Pasadena, CA 91109
†Division of Geological and Planetary Sciences, California Institute of Technology, Pasadena, CA 91109

***Abstract*— Aerial vehicles are appealing systems for possible future exploration of planets and moons such as Venus and Titan, because they combine extensive coverage with high-resolution data collection and in-situ science capabilities. Recent studies have proposed the use of a montgolfiere balloon, which controls its altitude by changing the heating rate or venting gas from the balloon, but has no actuation capability in the horizontal plane. A montgolfiere can use the variation in wind with altitude to guide itself to a desired location. This paper considers the problems of determining the altitude profile that the montgolfiere should follow in order to reach its target most quickly. We provide a new method that solves this path planning problem for all possible target locations, thereby providing a reachability analysis for the entire globe. The key idea is to perform a principled simplification and decoupling of the dynamics of the montgolfiere. We then discretize the search space, converting the planning problem into a graph search problem, and use Dijkstra's algorithm to calculate the minimum-time path from the start location to every possible location in the graph. We demonstrate the approach on a possible Titan mission scenario.**

I. Introduction

Previous planetary missions have been explored using orbiters, landers and ground-based rovers. Orbiters can provide low-to-medium resolution imagery over a limited number of spectral bands, and have limited capabilities when the planetary atmosphere is opaque. Landers and rovers can provide high-resolution imagery and in-situ data collection, but have coverage limited to a single site (in the case of a lander) or to a few kilometers (for rovers)[1]. There is therefore a need for exploration technologies that can combine extensive coverage with high-resolution data collection and in-situ science capabilities. In the case of planets and moons with atmospheres, such as Titan and Venus, a number of authors have proposed the use of aerial systems to fulfill this need[1], [2], [3], [4]. Lighter-than-atmosphere (LTA) systems are particularly appealing, since the energy required to keep them airborne is small.

Recent studies have proposed the use of a montgolfiere balloon for possible exploration of Titan, Mars and Venus[2], [3], [4]. One of NASA's Outer Planet Flagship mission concepts currently under consideration is the Titan Saturn System Mission (TSSM), which would be a joint NASA-ESA partnership that plans to employ a montgolfiere along with a lake lander and an orbiter[5]. This montgolfiere would circle Titan, investigating how Titan and Saturn operate as a system and determining how far prebiotic chemistry has developed. The planned launch date for the TSSM concept is 2020.

A montgolfiere, also known as a hot air balloon, maintains buoyancy by heating the atmospheric gas inside the balloon. Such a balloon can control its altitude by changing the heating rate or venting gas from the balloon, but has no actuation capability in the horizontal plane. The motion of the montgolfiere in the horizontal plane is driven by the local winds. Conceptually, however, it may be possible for the balloon to use the difference in winds at different altitudes to guide itself to a desired location. Such an approach would rely on predictive models of the winds on a planet or moon. These models are known as General Circulation Models, and in recent years much attention has been devoted to their development, for example [6], [7], [8], [9], [10], [11], [12], [13]. In our research we have chosen to make use of the work of [6], who developed a general purpose numerical model of planetary atmospheric and climate dynamics known as PlanetWRF. This general model has been specialized to generate global, time-varying, three-dimensional wind models for Mars, Titan and Venus. Further development of these models is an ongoing research topic that we do not address in this paper. Instead we assume that such a model exists and can be considered accurate enough for the purposes of motion planning.

In this paper, we consider two related problems. The first is:

> "Given an initial position and target location, what altitude profile should the montgolfiere follow in order to reach its target most quickly?"

This is critical in enabling a montgolfiere to achieve the horizontal motion necessary for effective science return. The second question is:

> "Given an initial position, what points on the planet's surface can be reached, and in what time?"

This reachability analysis is critical in performing trade studies to determine the right aerial system to use, and where and when such a system should be deployed. For example, we need to answer questions such as whether a single 6-month Titan mission could reach both a given lake-filled area and the poles. The trades studies require that the reachability analysis is global, rather than local.

These problems are challenging for a number of reasons.

[1]Government sponsorship acknowledged.

The magnitude and direction of the wind field varies drastically depending on location and time, and this variation is highly nonlinear, due to the nonlinearity of the underlying models. At the same time, the horizontal motion of the montgolfiere is driven by the local wind velocity, which means that the wind cannot be considered as merely a disturbance. A common approach to deal with nonlinearities is linearization about a reference trajectory; however, finding a feasible reference trajectory is far from straightforward. In the case of a montgolfiere, feasible trajectories from one location to another are far from a straight line, and may even require significant motion away from the target in order to find winds that will eventually lead back to the goal.

In this paper we present a new method for reachability analysis with montgolfieres that solves both the problems of path planning and reachability. The new method first performs a principled simplification and decoupling of the dynamics of the montgolfiere. This enables us to perform an efficient discretization of the search space, converting the planning problem into a graph search problem. We then use Dijkstra's algorithm to calculate the minimum-time path from the start location to every possible location in the graph. This solves the reachability problem, and then, for a given desired location, we can extract the minimum-time altitude profile to the goal, thereby solving the path planning problem. These solutions are approximate, due to the discretization used in generating the graph. Since the reachability results are intended for early trade studies that require accuracy in 100s of kilometers, and not for accurate placement of the balloon, approximation error is tolerable. The key requirement is that global reachability can be assessed. In flight the planned paths would be used as guidance trajectories, with a feedback controller being used to drive the state of the balloon to the planned trajectory in the face of disturbances, model uncertainties and approximation error. Design of a feedback controller for a montgolfiere is beyond the scope of this paper, and is a topic of current research by other authors.

The organization of this paper is as follows. We state the problem in Section III. The new approach is described in Section IV. In Section V we present two extensions to the approach, namely a decomposition approach that allows the approach to scale to problems with time-varying wind models, and a capability for revisiting science targets. In Section VI we show planned paths and reachability maps for a number of scenarios on Titan.

II. Related Work

The problem of path planning for montgolfieres was studied by [14], [15]. In [14], the authors assume that wind fields vary linearly in space and are fixed in time. Given this assumption, they solve the optimal control problem to find the sequence of heating inputs that takes the balloon from its initial state to the goal. The optimal control approach is inherently limited to linear wind fields, whereas the fields predicted by global circulation models are highly nonlinear. In our previous work we extended this approach to the case where the wind field consists of a discrete, finite set of layers, each of which has a constant wind direction and magnitude[15]. In this case the wind varies with altitude, but not with horizontal location. In the present paper we provide a new method that can handle arbitrary wind fields that vary nonlinearly in horizontal and vertical directions, as well as in time. Such a capability is necessary given that the available General Circulation Models predict a strong dependence of the winds on all three of these parameters.

A problem that has received considerable attention is that of path planning for autonomous underwater vehicles (AUVs) in current fields[16], [17], [18], [19], [20], [21]. While the AUVs are assumed to have significant horizontal actuation capabilities, the currents have a significant effect on the motion of the AUV, meaning that this problem shares some aspects of the montgolfiere path planning problem. The approach of [21] poses the path planning problem as a nonlinear optimization problem, and uses a 'swarm' of feasible paths to provide multiple initial guesses to an optimizer such as local random search, or simulated annealing. The performance of such optimizers is highly dependent on the quality of the initial guess, and in the montgolfiere case, finding feasible paths to use as guesses is very challenging. Alternative approaches use a spatial discretization approach combined with a variety of search techniques to solve the planning problem. [16] use a genetic algorithm to search for the optimal path in a two-dimensional field; however, this search algorithm does not guarantee convergence to a global (or even feasible) solution, and does not solve the reachability problem. [17] instead use A* graph search to guarantee that the optimal path is found; however, this work is restricted to a two-dimensional, time-invariant current field and assumes that the AUV has significant actuation capabilities in the horizontal plane. [18] use a fast-marching search technique to find optimal paths; however, these approaches can return infeasible plans if the current is stronger than the actuation capability of the AUV[20]. This is clearly the case with a montgolfiere, which has no horizontal actuation capability. [20] extends fast-marching techniques to the case where currents are stronger than actuators, however it is not clear that this extends to the case of a montgolfiere balloon; in addition [20] considers only the path planning problem and not the reachability problem.

III. Problem Statement

We assume that we have a general set of dynamic equations for the montgolfiere in a time-varying wind field of the form:

$$\dot{\mathbf{x}}(t) = f(\mathbf{x}(t), \mathbf{u}(t), t), \tag{1}$$

where $\mathbf{u}(t)$ are the heating and venting control inputs applied at time t, and $\mathbf{x}(t)$ is the state of the montgolfiere at time t. Equations in this form are derived by [14] using the thermal and dynamics balloon models of [22]. In this case, the state includes the temperature and volume of the balloon, as well as the three-dimensional position and velocity of the montgolfiere, which we denote $\mathbf{r}$ and $\dot{\mathbf{r}}$ respectively. The

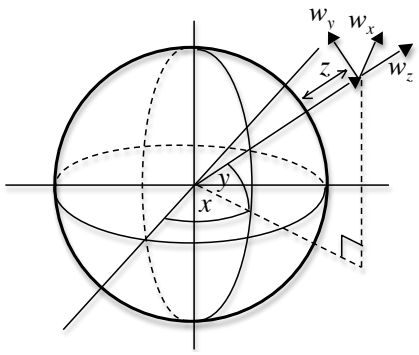

Fig. 1. Coordinate frame definitions. Degrees longitude is denoted x, degrees latitude is denoted y and z is the altitude from the surface of the planet. The velocities w_x, w_y and w_z are defined in a Cartesian coordinate frame fixed to the local surface tangent.

dynamics in (1) rely on a predictive model of the winds at any location $\mathbf{r}$ and time t. We assume we have such a model in the general form $\mathbf{w}(\mathbf{r}, t)$. Here, position is defined in a spherical coordinate frame such that:

$$\mathbf{r} \triangleq \begin{bmatrix} x \\ y \\ z \end{bmatrix}, \tag{2}$$

where x is in degrees longitude, y is in degrees latitude, and z is altitude from the surface of the planet. Wind velocity is defined in a Cartesian coordinate frame fixed to the local surface tangent such that:

$$\mathbf{w}(\mathbf{r}, t) \triangleq \begin{bmatrix} w_x(\mathbf{r}, t) \\ w_y(\mathbf{r}, t) \\ w_z(\mathbf{r}, t) \end{bmatrix}, \tag{3}$$

where w_x, w_y and w_z are the velocities in the easterly, northerly and vertically upwards directions respectively. The coordinate frames are shown in Figure 1.

The path planning and reachability problem may now be stated as follows:

Problem 1. *Given a montgolfiere with dynamics $f(\cdot)$ initially at location $\mathbf{r}_0$, and a wind model $\mathbf{w}(\cdot)$, determine, for every possible end location $\mathbf{r}_f$, the minimum time to reach $\mathbf{r}_f$ and the sequence of control inputs $\mathbf{u}(\cdot)$ that achieves this minimum.*

In the following section we describe our approach to solving a discretized version of this problem.

IV. Graph Search for Montgolfiere Path Planning and Reachability

A. Overview

The new approach for montgolfiere path planning consists of three steps:

1) Perform a principled decoupling and simplification of the montgolfiere dynamics
2) Generate a graph using a spatial and temporal discretization of search space
3) Find optimal paths and reachability using Dijsktra's algorithm[23]

These steps are described in detail in Sections IV-B through IV-D. The choice of a discretized search space is motivated by the observation that, in the case of the montgolfiere, the dynamics of the balloon in the horizontal plane are entirely driven by the wind field. It is therefore essential to capture the nonlinear spatial and temporal variability of the wind field as fully as possible; Restricting our attention to an analytically convenient form of wind field (such as a linear field) is not appropriate. At the same time, we need to perform global path planning and reachability analysis. Both of these can be achieved using a discretized search space combined with graph search; the decoupling in Step 1 uses the structure of the montgolfiere dynamics to make this discretization efficient. In this section we restrict our attention to wind fields that are fixed in time at $t = T$; the extension to time-varying fields is described in Section V-B.

B. Simplification and Decoupling of Dynamics

The montgolfiere planning problem is more complex than the problems considered in [16], [17], [18], [19], [20], [21] because it takes place in a three-dimensional environment. We can, however, simplify the problem using a partial decoupling of the montgolfiere dynamics. This decoupling is based on the following assumptions:

Assumption 1. *The altitude of the montgolfiere is fully controllable, subject to maximum rise and sink rates, denoted v_{rise} and v_{sink} respectively.*

Assumption 2. *The horizontal velocity of the montgolfiere is proportional to the local horizontal wind velocity at all times.*

Assumption 1 comes from the observation that the vertical control authority of the montgolfiere is large compared to the vertical winds predicted by the global circulation models of [6]. This means we can assume that a separate altitude controller exists that issues heating and venting commands to reject wind disturbances and to drive the montgolfiere to a desired altitude setpoint. This allows us to ignore the effects of vertical winds and the complicated thermodynamic model used by [14] to described the vertical motion of the montgolfiere. As long as accurate altitude measurements are available, the existence of such a controller is a mild assumption; standard approaches such as PID will typically be sufficient to drive the altitude error to zero.

Assumption 2 comes from [14], who use the following relationship for the horizontal dynamics of the montgolfiere:

$$\dot{x} = \gamma \cdot w_x(x, y, z) \qquad \dot{y} = \gamma \cdot w_y(x, y, z), \tag{4}$$

where γ is a measure of the drag of the montgolfiere in the horizontal plane. These dynamics mean that, in the horizontal plan, we need *only* consider the local wind velocity. We do not need to consider any other thermal or dynamic state of the montgolfiere. This simplification, along with that given by Assumption 1 is critical in efficiently generating a discretized graph, as described in the following section.

C. Graph Generation

The graph generation problem may be stated as follows:

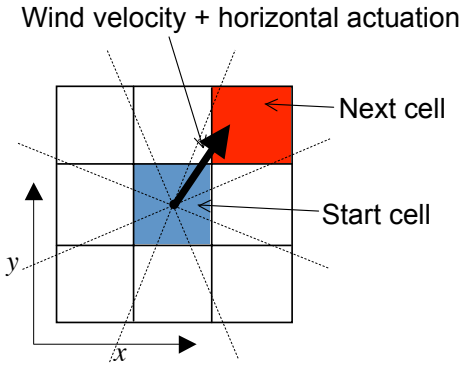

Fig. 2. Discretization in the horizontal plane.

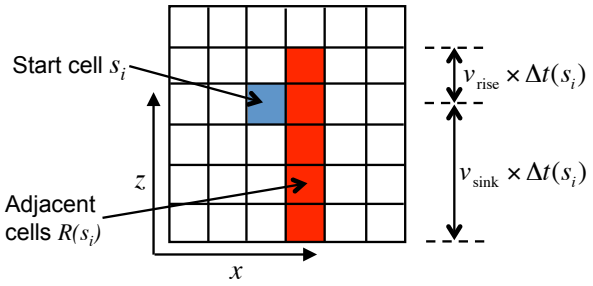

Fig. 3. Discretization in the vertical plane.

Problem 2. *Generate a graph $\mathcal{G}$ consisting of a set of nodes $\mathcal{S}$, where each node $s_i \in \mathcal{S}$ consists of an index i and a position $\mathbf{r}(s_i)$, a set of arcs between nodes, and an adjacency matrix A defined such that $A(i,j)$ is the cost to traverse the arc from s_i to s_j. $A(i,j) = \infty$ implies that no arc exists between s_i and s_j.*

In generating the nodes, we choose to discretize space using a uniform grid, where adjacent nodes are separated by Δx in longitude, Δy in latitude, and Δz in altitude. The decoupling described in Section IV-B enables us to consider the discretization of the three-dimensional search space first in the horizontal plane, and then in the vertical plane. The adjacency matrix A is populated as follows. For every node s_i, known as the source node, we use the wind model to determine the local wind $\mathbf{w}(\mathbf{r}(s_i), T)$. Considering the horizontal plane first, from (4), the horizontal velocity of the montgolfiere is in the same direction as that of the local wind. We discretize the direction of the montgolfiere velocity in the horizontal plane into one of eight segments, as shown in Figure 2. Which of these segments the local wind velocity falls into determines the cell that the montgolfiere will transition to if no vertical actuation is applied, which we denote s_i'. By assuming that the wind is constant in the interval until the next cell is reached, the time taken to travel from s_i to s_i' is given by:

$$\Delta t(s_i) = \frac{dist(\mathbf{r}(s_i), \mathbf{r}(s_i'))}{||\mathbf{w}(\mathbf{r}(s_i), T)||}. \tag{5}$$

Here, $dist(\cdot,\cdot)$ is a function that returns the cartesian distance between two points in a spherical coordinate frame, while $||\cdot||$ is the standard vector 2-norm.

By applying vertical actuation, cells above or below s_k may also be reached. By Assumption 1, the vertical range of the montgolfiere depends only on the maximum rise and sink rates and the time available. Hence the maximum altitude increase and decrease possible in traveling from s_i to an adjacent cell are:

$$z_{\text{rise}}(s_i) = \frac{v_{\text{rise}}}{\Delta t(s_i)} \qquad z_{\text{sink}}(s_i) = \frac{v_{\text{sink}}}{\Delta t(s_i)}. \tag{6}$$

The set of cells $\mathcal{R}(s_i)$ for which an arc exists between s_i and $s_j \in \mathcal{R}(s_i)$ is therefore given by:

$$s_j \in \mathcal{R}(s_i) \iff \begin{cases} x(s_j) = x(s_i') \\ y(s_j) = y(s_i') \\ z(s_i') - z_{\text{sink}} \leq z(s_j) \leq z(s_i') + z_{\text{rise}}(s_i). \end{cases} \tag{7}$$

We can now populate the adjacency matrix A. Since Problem 1 requires us to find the minimum time to get from every node to every other node, the cost on an arc must be the time taken to traverse that arc. The matrix A is therefore populated as follows:

$$A(i,j) = \begin{cases} \Delta t(s_i) & s_j \in \mathcal{R}(s_i) \\ \infty & s_j \notin \mathcal{R}(s_i). \end{cases} \tag{8}$$

Notice that, even though we have discretized space and wind direction, we have retained time and wind magnitude as continuous variables. This ensures that arbitrarily large variations in wind magnitude can be captured without requiring an intractably large number of grid cells. This is essential, since the PlanetWRF wind model predicts winds that vary in magnitude over several orders of magnitude.

D. Graph Search

Given a graph $\mathcal{G}$, Dijkstra's algorithm[23] finds the minimum cost path from a start node to all other nodes in the graph. The running time of Dijkstra's algorithm scales with the square of the number of nodes, and is hence an appealing algorithm even for large graphs. In this paper we use Dijkstra's algorithm to find the minimum-time path between the node nearest to the initial location of the montgolfiere, denoted s_i, and all other nodes. This solves a discretized approximation to the reachability problem. Given the reachability results, the path planning problem can be solved simply, by extracting the path $p \in \mathbb{Z}^N$ corresponding to the particular target node s_l. This path consists of a sequence of node indices such that $p(1) = i$ and $p(N) = l$. The altitude profile to be followed by the montgolfiere to reach its goal in minimum time is then given by:

$$\mathcal{P} = [z(s_p(1))\ z(s_p(2))\ \ldots\ z(s_p(N))]. \tag{9}$$

We have assumed, consistent with Assumption 1, that the altitude of the montgolfiere is regulated by a controller

issuing heating and venting commands. Since the altitude profile $\mathcal{P}$ is consistent with the maximum rise and sink rates of the montgolfiere, we have solved the discretized version of the path planning problem.

V. Enhancements to Algorithm

A. Loitering

The preceding methods enable path planning for the montgolfiere to reach the location of a desired science target. Once arrived at the target, however, the lack of horizontal actuation presents a new problem: "how long could we remain in one cell to perform science observations?" One obvious solution - dropping an anchor - might not be practical from altitude and mass considerations. Instead we consider again using the wind field predictions. If the altitude is not constrained, then we could position the montgolfiere at the altitude of smallest predicted horizontal wind magnitude, or equivalently, to the altitude containing the longest duration adjacency arc $A(i,j)$. Some typical results for Titan are given in Section VI.

Eventually, the montgolfiere would drift out of the science target cell. If the mission requires further observations of the target cell, it would be useful to determine if the montgolfiere could repeatedly return to the same cell given the predicted wind fields; i.e., find the shortest time or distance cycle path that includes the science target cell. For the general case of locating cycles in a directed graph, there are reported methods available, for example [24], [25]. However, for our case we know the initial science target cell, s_i, which means that a more straightforward approach is feasible:

1) Determine $\mathcal{R}(s_i)$, the set of cells adjacent (reachable in one step) to s_i using (7).
2) For each adjacent cell $s_j \in \mathcal{R}(s_i)$, run the existing shortest path finder with s_i as the end goal.

If the science target requires us to be at a particular altitude, then the altitude of s_i would be fixed. In this case we must perform a path search for each of the m adjacent nodes, where m is the cardinality of $\mathcal{R}(s_i)$). If, instead, we can search over all altitudes to find the minimum-time cycle, then we must also perform path searches for all of the L possible altitudes. However, due to the overlap of the adjacent nodes, in the worst case we have to perform only $8L$ path searches. We can further reduce the graph size by adding distance or time constraints. Assuming the montgolfiere must return to s_i within a desired time T_d, or travel no farther from s_i than distance D, then we can first determine the reachability map from s_i as the starting point, then remove all cells from the graph that are farther than T_d in time, or D in distance, before searching the remaining graph for the shortest possible cycles. In Section VI we present some examples of loitering on Titan.

B. Time-Varying Wind

Up to the previous section, the wind field is assumed to be static. This section extends the approach in Section IV to time-varying wind fields.

Because the wind at a given location differs depending on when the balloon reaches there, each node s_i in the graph now corresponds to a time t_i as well as a position $\mathbf{r}(s_i)$. This increases the dimension of the discretized grid environment from 3 to 4. Time is discretized with a step size dt. Let n_x, n_y, n_z, and n_t denote the number of cells in x, y, z, and t axes, respectively. Let $n_r = n_x n_y n_z$ denote the number of cell positions in the environment. Then, by adding the time axis to the graph, the size of the adjacency matrix A increases from $n_r \times n_r$ to $n_r n_t \times n_r n_t$.

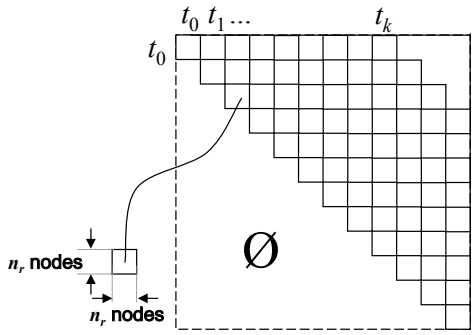

Fig. 4. Adjacency matrix in the case with the time-varying wind field.

As with the static wind case, the first step of the graph construction is to find which horizontal neighboring cell the balloon will reach from each cell. In the static wind case, the wind direction at the cell center determines which neighboring cell the balloon will hit. In the time-varying case, however, to handle the nonlinear wind field the wind vector is numerically integrated over time from the center of each cell s_i until the integrated position reaches one of the neighboring cells s_i'. This gives the time of travel $\Delta t(s_i)$ from s_i to s_i'. To account for a continually weak wind field in which the balloon cannot reach a neighboring cell, the integration is terminated at time $k\,dt$, so that $\Delta t(s_i) \le k\,dt$. In such a case, the vehicle is assumed to stay in the same cell for a duration of one time step dt, reaching another node s_i' with the same position but a different time. The rest of the graph construction procedure is the same as the one presented in Section IV-C, except the adjacency set definition (7) is replaced with:

$$s_j \in \mathcal{R}(s_i) \Leftrightarrow \begin{cases} x(s_j) = x(s_i') \\ y(s_j) = y(s_i') \\ z(s_i') - z_{\text{sink}}(s_i') \le z(s_j) \le z(s_i') + z_{\text{rise}}(s_i') \\ |t(s_i) + \Delta t(s_i) - t(s_j)| \le dt. \end{cases}$$

Because the balloon only moves in the positive direction in time, the adjacency matrix can be represented by an upper block-triangular matrix, by ordering the cells by their time t_i, as shown in Figure 4. Each block contains a snapshot of the world, whose size is n_r by n_r.

As the size of the graph increases, the memory requirement for graph construction and Dijkstra's algorithm becomes significant. However, the upper block-triangular structure of the adjacency matrix can be exploited to decompose the problem into several smaller subproblems, requiring

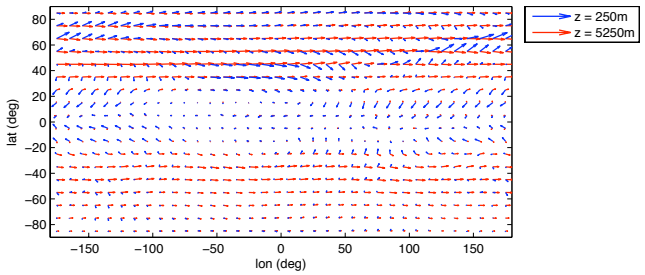

Fig. 5. Example of winds generated using Titan General Circulation Model.

much smaller memory. The details are beyond the scope of the paper and omitted here.

VI. Application Examples

All the algorithms are implemented in MATLAB. The results in this section were generated using the wind field model of Titan developed by [6]. The following parameters were used:

$$\begin{aligned} n_x &= 36 && (\Delta x = 10 \text{ [deg]}) \\ n_y &= 18 && (\Delta y = 10 \text{ [deg]}) \\ n_z &= 20 && (\Delta z = 500 \text{ [m]}) \\ n_t &= 520 && (dt = 0.02 \text{ [titan day]} \\ k &= 100 \\ \gamma &= 1.0 \end{aligned}$$

Thus, $n_r = 12960$ in Figure 4. Figure 5 shows two examples of wind fields generated using this model. Note that the magnitude and direction of the wind field varies greatly with location.

A. Loitering

Figure 6 illustrates predicted minimum velocities and longest hover times for a fixed wind field on Titan.

Figure 7 illustrates the loitering capability presented in Section V-A. Here we assumed a deterministic and stationary wind field, but the method is straightforward to extend to nonstationary wind field models. Figure 7 shows the shortest duration cycles to return to six sites of scientific interest on Titan, as well as the duration of the shortest cycle from each cell on the globe.

B. Time-varying Wind

This subsection shows simulation results with a time-varying wind field. The starting altitude is set to be $5000m$.

Figures 8 show reachability plots from different starting locations to all the cells at altitude $250m$. The starting cell is marked with "S". The color of each cell shows the time it takes to move from the start to each cell.

Note that depending on where the balloon starts, the reachability map varies significantly. Figures 8(a) and 8(b) show that it is difficult to reach areas around the southern pole if we start further North. This is explained by the fact that the wind in the north-south direction is generally weak near the southern pole.

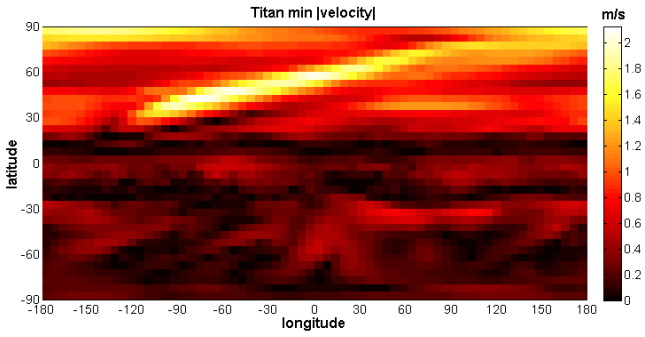

(a)

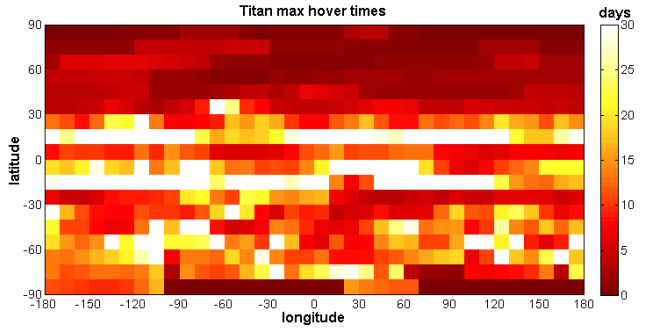

(b)

Fig. 6. Titan wind field (a) minimum horizontal velocities and (b) maximum hover times.

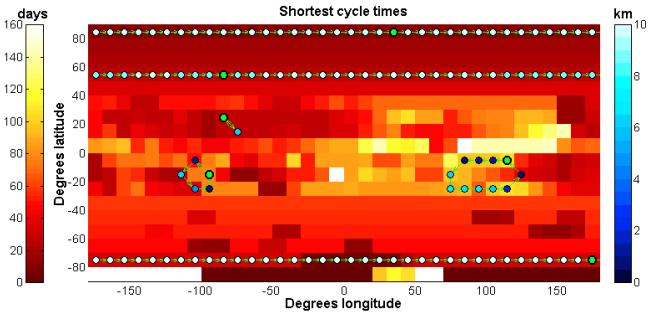

Fig. 7. Illustration of loitering capability on Titan. The background color indicates the number of days in the shortest cycle starting in each cell. The shortest cycles are shown for six difference science targets (green circles). The colored circles indicate commanded altitude.

Figure 9 shows the percentage of the area of Titan's surface that would be reachable in a given time. For example, 50% on the y axis means that 50% of the points on Titan's surface could be reached in a given time if set as a destination of the shortest path problem[1]. The plot has 24 different starting locations with the following combination of longitude and latitude.

- 4 longitudes (175°W, 85°W, 5°E, 95°E)
- 6 latitudes (85°S, 45°S, 15°S, 15°N, 45°N, 85°N)

Because the wind field changes over the latitude much more than the longitude, the lines corresponding to the same latitude are plotted with the same color. In fact, the lines

[1]Note that this is *not* a coverage plot, which would give the time taken for the montgolfiere to sweep over 50% of Titan's surface.

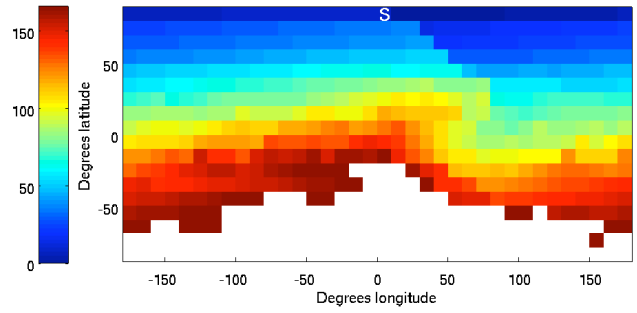

(a) From 85 degrees north, 5 degrees east

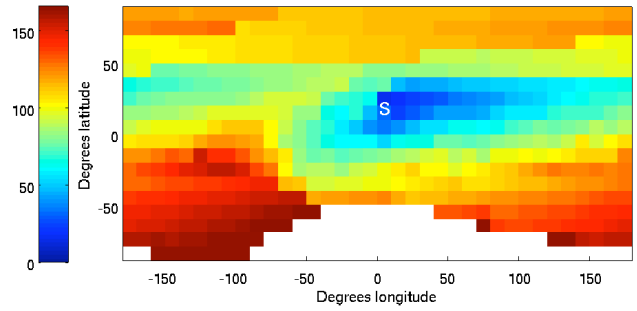

(b) From 15 degrees north, 5 degrees east

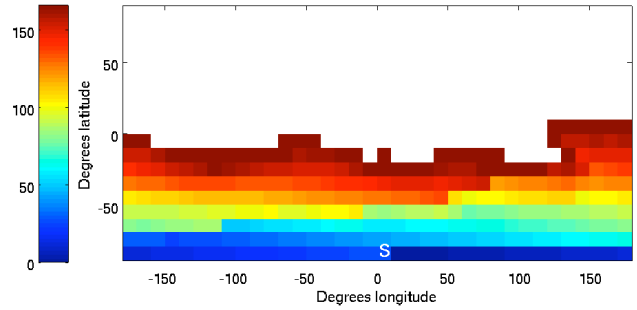

(c) From 85 degrees south, 5 degrees east

Fig. 8. Reachability plots from three different starting locations. The color bar on the left shows the time to reach each cell (in days). A white cell is unreachable.

with the same color have a similar trend: if the balloon starts at 15°S (shown in red), it could initially reach only limited areas, but the reachable area grows rapidly after a few months; if the balloon starts near the southern pole (85°S), it could reach a very limited area in 5 months. This is because the north-south wind near the southern pole is weak.

Figure 10 shows several trajectories from a start location of (15°N, 5°E) to 3 different destinations (5°S, 165°E), (75°S, 85°W), and (85°N, 85°E). The size of the circles represent the elapsed time from start, and the color of the circles represent the altitude of the trajectory. The background color represents the same reachability map as was shown in Figure 8(b), but the colormap is changed to better highlight the altitude change. Note that because of the nonlinear and time-varying wind field, the minimum-time trajectories involve large changes in altitude and are far from being straight lines.

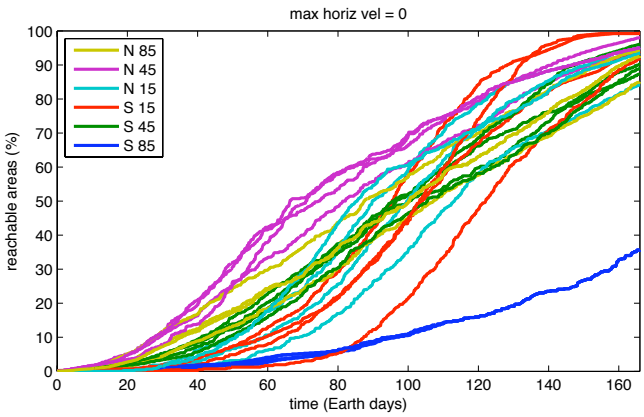

Fig. 9. The area that could be reached as a function of time.

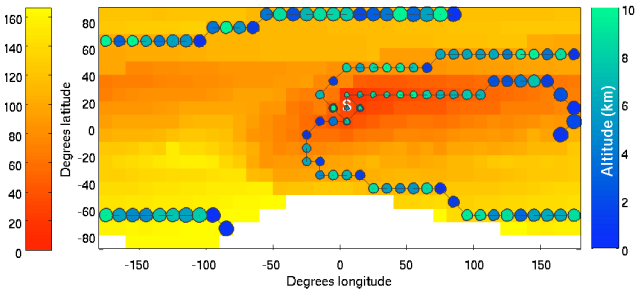

Fig. 10. The trajectories from a start to 3 different destinations. The left color bar shows the time to reach the destination cell. The right color bar shows the altitude of the trajectory. The size of the circle shows elapsed time along a particular trajectory.

VII. Conclusion

In this paper we have presented a new method for global path planning with montgolfiere balloons. The planning approach enables a montgolfiere to exploit variations in the wind field at different altitudes to achieve a desired horizontal motion. By using a spatial and temporal discretization combined with existing graph search techniques we can determine the altitude profiles that reach a target in minimum time, and can determine the set of all reachable targets from a given start location. We presented example results from Titan using the wind field model of [6]. Future work will investigate the approximation error introduced by the new approach, and how this approximation error can be mitigated by the use of a feedback controller.

Acknowledgment

The research described in this paper was carried out at the Jet Propulsion Laboratory, California Institute of Technology, under a contract with the National Aeronautics and Space Administration.

References

[1] A. Elfes, J. L. Hall, J. F. Montgomery, C. F. Bergh, and B. A. Dudik, "Towards a substantially autonomous aerobot for exploration of Titan," in *Proceedings of the IEEE International Conference on Robotics and Automation*, 2004.

[2] J. Jones, "Montgolfiere balloon missions from Mars and Titan," in *Proceedings of the 3rd International Planetary Probe Workshop*, 2005.

[3] J. O. Elliott, K. Reh, and T. Spilker, "Concept for Titan exploration using a radioisotopically heated montgolfiere," in *Proceedings of the IEEE Aerospace Conference*, 2007.
[4] D. Fairbrother, "Development of planetary ballooms," in *Proceedings of the NASA Space Technology Conference*, 2007.
[5] NASA, "Outer planet flagship mission: Titan saturn system mission (tssm)," http://opfm.jpl.nasa.gov/titansaturnsystemmissiontssm/.
[6] M. I. Richardson, A. D. Toigo, and C. E. Newman, "PlanetWRF: A general purpose, local to global numerical model for planetary atmospheric and climate dynamics," *Journal of Geophysical Research*, vol. 112, 2007.
[7] R. M. Haberle, M. M. Joshi, J. R. Murphy, J. R. Barnes, J. T. Schofield, G. Wilson, M. Lopez-Valverde, J. L. Hollingsworth, A. F. C. Bridge, and J. Schaeffer, "General circulation model simulations of the mars pathfinder atmospheric structure investigation/meteorology data," *Journal of Geophysical Research*, vol. 104, pp. 8597–8974, 1999.
[8] S. R. Lewis, M. Collins, P. L. Read, F. Forget, F. Hourdin, R. Fournier, C. Hourdin, O. Talagrand, and J. P. Huot, "A climate database for mars," *Journal of Geophysical Research*, vol. 104, pp. 24 177–24 194, 1999.
[9] Y. O. Takahashi, H. Fujiwara, H. Fukunishi, M. Odaka, and Y. Hayashi, "Topographically induced north-south asymmetry of the meridional circulation in the martian atmosphere," *Journal of Geophysical Research*, vol. 108, 2003.
[10] T. Tokano, F. M. Neubauer, M. Laube, and C. P. McKay, "Seasonal variation of Titans atmospheric structure simulated by a general circulation model," *Planet. Space Sci.*, vol. 47, pp. 493–520, 1999.
[11] D. F. Luz, F. Hourdin, P. Rannou, and S. Lebonnois, "Latitudinal transport by barotropic waves in Titans stratosphere. ii. results from a coupled dynamics-microphysics-photochemistry gcm," *Icarus*, vol. 166, no. 2, pp. 343–358, 2003.
[12] M. Yamamoto and M. Takahashi, "The fully developed superrotation simulated by a general circulation model of a Venus-like atmosphere," *J. Atmos. Sci.*, vol. 60, no. 3, pp. 561–574, 2003.
[13] C. Lee, S. R. Lewis, and P. L. Read, "A numerical model of the atmosphere of Venus," *Adv. Space Res.*, vol. 11, no. 36, pp. 2142–2145, 2005.
[14] T. Das, R. Mukerjee, and J. Cameron, "Optimal trajectory planning for hot-air balloons in linear wind fields," *AIAA Journal of Guidance, Control and Dynamics*, vol. 3, no. 26, pp. 416–424, 2003.
[15] T. Kämpke and A. Elfes, "Optimal wind-assisted flight planning for planetary aerobots," in *Proceedings of the International Conference on Robotics and Automation*, 2004.
[16] A. Alvarez, A. Caiti, and R. Onken, "Evolutionary path planning for autonomous underwater vehicles in a variable ocean," *IEEE Journal of Ocean Engineering*, vol. 2, no. 29, pp. 418–429, 2004.
[17] B. Garau, A. Alvarez, and G. Oliver, "Path planning of autonomous underwater vehicles in current fields with complex spatial variability: an A* approach," in *Proceedings of the International Conference on Robotics and Automation*, 2005.
[18] C. Petres, Y. Pailhas, P. Patron, Y. Petillot, J. Evans, and D. Lane., "Path planning for autonomous underwater vehicles," *IEEE Transactions on Robotics*, vol. 2, no. 23, pp. 331–341, 2007.
[19] D. Kruger, R. Stolkin, A. Blum, and J. Briganti, "Optimal AUV path planning for extended missions in complex, fast-flowing estuarine environments," in *Proceedings of the International Conference on Robotics and Automation*, 2007.
[20] M. Soulignac, P. Taillibert, and M. Rueher, "Adapting the wavefront expansion in presence of strong currents," in *Proceedings of the International Conference on Robotics and Automation*, 2008.
[21] J. Witt and M. Dunbabin, "Go with the flow: Optimal AUV path planning in coastal environments," in *Proceedings of the Australasian Conference on Robotics and Automation*, 2008.
[22] L. A. Carlson and W. J. Horn, "New thermal and trajectory model for high-altitude balloons," *Journal of Aircraft*, vol. 20, no. 6, pp. 500–507, 1983.
[23] E. W. Dijkstra, "A note on two problems in connexion with graphs," *Numerische Mathematik*, vol. 1, pp. 269–271, 1959.
[24] R. W. Floyd, "Non-deterministic algorithms," *Journal of the Association for Computing Machinery*, vol. 14, no. 4, pp. 636–644, 1967.
[25] R. P. Brent, "An improved monte-carlo factorization algorithm," *BIT Numerical Mathematics*, vol. 20, no. 2, pp. 176–184, 1980.